Original Paper

Eletrônica de Potência
Open Journal of Power Electronics

Received August 13, 2025; Received in revised form October 10, 2025, November 26, 2025; Accepted December 16, 2025; Date of publication January 14, 2025.
The review of this paper was arranged by Associate Editor Wilmar P. Castiblanco and Editor-in-Chief Allan F. Cupertino.
Digital Object Identifier http://doi.org/10.18618/REP.e202605

Bayesian Optimization-Based Tuning of the Proportional-Integral Controller for Grid-Connected Three-Level NPC Converter

Vitor S. Jorge[1,*], Angelo S. Lunardi[1,2], Luan A. Sousa[2], Rodolfo V. Rocha[1,2,3], Renato M. Monaro[2], and Alfeu J. Sguarezi Filho[1,2]

[1]Federal University of ABC, Center for Engineering, Modeling and Applied Social Sciences, Santo André, São Paulo 09210-580, Brazil.
[2]University of São Paulo, São Paulo, São Paulo 05508-060, Brazil.
[3]Federal University of Mato Grosso, Cuiabá, Mato Grosso 78060-900, Brazil.

e-mail: jorge.vitor@ufabc.edu.br*; angelo.lunardi@ufabc.edu.br; luan.sousa@usp.br; rodolfo.rocha@ufmt.br; monaro@usp.br; alfeu.sguarezi@ufabc.edu.br.
*Corresponding author.

ABSTRACT Power converters provide energy interface in various applications; in photovoltaics, they interconnect solar panels to the grid, with two-level inverters being the most common across virtually all power ranges, followed by three-level neutral point clamped (3LNPC) converters. The proportional-integral (PI) controller is the most commonly employed controller for these converters. This paper proposes the use of Bayesian Optimization (BO) to tune the PI controller for a 3LNPC converter connected to the grid. The optimization algorithm was used to determine the controller's tuning gains through computational simulation. Subsequently, the PI controller tuned using BO was implemented on an experimental test bench to validate the concept. The performance of the controller tuned with the proposed method was compared to PI controllers adjusted using classical methods widely found in the literature. The test results demonstrated that Bayesian Optimization is straightforward to implement and, when compared to the Genetic Algorithm (GA), it exhibited a more effective and targeted exploration of the search space. This led to superior PI controller tuning, with improved dynamic response and reduced total harmonic distortion relative to the benchmark methods.

KEYWORDS Power converters, three-level, neutral point clamped, PI controller, Bayesian Optimization.

I. INTRODUCTION

Nowadays, several research studies in power generation focus on renewable energy systems (RES) due to the need to reduce greenhouse gas emissions [1]. These sources require power electronics for integration and control of the generated energy. The three-level Neutral Point Clamped (3LNPC) converter is the most typical multilevel topology found in renewable generation systems [2], [3]. These converters are mainly used in variable-speed wind turbines but are also applied in pumped hydro energy storage plants [4], [5]. For this reason, the 3LNPC converter is the subject of study in this paper, given its great potential and application in variable-speed generation systems [6]–[8].

Voltage Source Converters (VSCs) play a fundamental role in grid-connected systems, enabling efficient electrical energy conversion. However, the presence of nonlinear loads can degrade voltage quality, introducing harmonics and affecting system stability. To mitigate these effects, controllers are integrated into VSCs, ensuring more precise operation [9]–[11]. Among the most widely used control methods, the Proportional-Integral (PI) controller stands out for its simplicity and effectiveness in compensating static and dynamic errors. However, its performance depends on the proper tuning of the controller parameters, requiring a deep understanding of the system's dynamic behavior [12]. The PI controller is designed to operate at a specific working point of the plant, where its gains are adjusted to optimize stability and dynamic response. Nevertheless, variations in operating conditions, such as load changes, external disturbances, or shifts in the operating point, can compromise its performance [13], [14]. These challenges necessitate advanced adaptive tuning techniques to ensure control robustness in dynamic environments.

Given the problem presented, several strategies have been developed for tuning the parameters of the PI controller. Among the classical methods, the Symmetrical Optimum (SO) is widely used. This method employs an approximate transfer function of the system to determine the gains that best adjust the controller. Its effectiveness depends on the accuracy of the system parameters, but variations in the plant gain and time constants can compromise the optimized calibration of the PI controller [15], [16]. In [17], a tuning method based on a first-order transfer function is proposed, where the controller gains are defined by the closed-loop

poles to ensure stability and good dynamic response. Although simple, this approach requires frequent adjustments if the plant parameters change over time.

Among computational intelligence methods, metaheuristic algorithms have been widely applied to PI controller tuning. Artificial Neural Networks (ANNs) are effective in this process as they can learn complex patterns and dynamically adapt controller parameters, as demonstrated in [18] for the control of a two-level grid-connected converter. However, ANNs require high computational power and a large volume of data for efficient training [19], [20]. The Genetic Algorithm (GA) is applied in [21] for PI tuning in a two-level grid-connected converter, offering a flexible approach capable of exploring a broad solution space and providing optimized tuning. However, algorithm tuning can be complex, and the computational cost is high [22]. The Grey Wolf Optimizer (GWO) efficiently adjusts PI controller gains in [23] for the control of a two-level grid-connected converter in an offshore wind system. This algorithm balances exploration and exploitation, but its application to highly nonlinear systems may be limited [24], [25].

The Whale Optimization Algorithm (WOA), applied in [26] for PI tuning in two-level converter control, is a simple and effective alternative for optimizing PI controller parameters. However, its sensitivity to parameter selection may affect the stability of the solution [27], [28]. The Particle Swarm Optimization (PSO) is a fast and easy-to-implement method, as evidenced in [29] for PI tuning in a grid-connected wind-solar cogeneration system. However, it may converge to local minima in complex systems [30], [31]. In [32], self-tuned PI controllers based on fuzzy logic are applied in a photovoltaic system. Unlike the previously mentioned methods, fuzzy logic is a heuristic approach that enables handling uncertainties and imprecisions, making it useful in control systems and artificial intelligence. However, properly tuning fuzzy sets can be a challenge [33], [34]. Finally, Bayesian Optimization (BO) is a probabilistic and iterative method that stands out for its efficiency in searching for optimal solutions in complex objective functions with high computational cost [35], [36]. Unlike the aforementioned algorithms, BO requires fewer data for tuning, avoids local minima, and efficiently handles high-dimensional problems, ensuring more effective convergence. Although it has been widely applied to predictive controller tuning, as in [37] and [38], this strategy has not yet been extensively explored for the PI controller tuning applied to 3LNPC converters.

Within this context, this paper aims to evaluate the Bayesian Optimization (BO) method in PI controller tuning for current control of a grid-connected 3LNPC converter. An experimental platform, consisting of a real grid-connected 3LNPC converter, is used to compare the performance of traditional PI tuning methods with the Bayesian Optimization-based approach, assessing the effectiveness and robustness of each technique in controller parameter adjustment. The main contributions of the article are as follows:

- Improved PI Controller Tuning: The Bayesian Optimization (BO) algorithm applied to PI controller tuning finds the gains more quickly and efficiently. As an iterative method, the algorithm can provide multiple sets of gains that ensure good performance in controller tuning;
- Superior Dynamic Performance: The controller tuned with BO-optimized gains exhibits lower overshoot, reduced steady-state error, and shorter settling time compared to controllers tuned using classical methods (SO and Yazdani);
- Novel Contribution: This study addresses a gap in the literature by exploring the application of Bayesian Optimization in PI controller tuning for the 3LNPC converter.

This work is divided as following: Section II presents the proposed methodology, the modeling of the PI controller for the 3LNPC converter, and the tuning using BO. Section III introduces the experimental setup used to validate the controller tuning. In Section IV, the results of the BO-based tuning and experimental validation are presented. Finally, Section V concludes the study.

II. PROPOSED METHODOLOGY

This work proposes the use of Bayesian Optimization as a tuning method for the PI controller applied to the control of a 3LNPC converter. The approach employs an offline simulation of the model to implement the BO process and determine the controller's tuning gains. Subsequently, these gains are used for configuring the controller applied in an experimental bench setup. Fig. 1 presents the complete framework of the proposed methodology. The following sections describe the grid-connected 3LNPC converter model, the implemented controller, and the Bayesian optimization process.

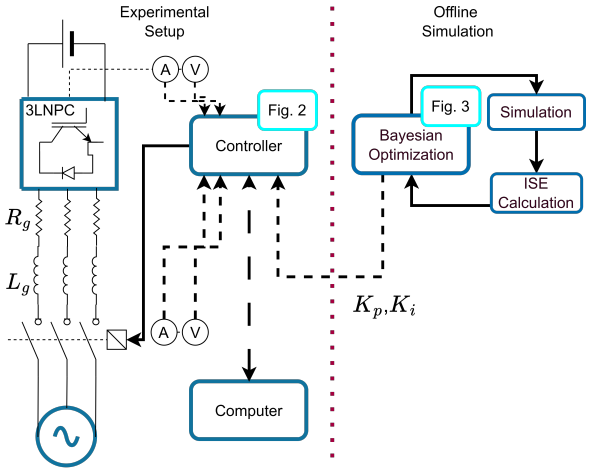

FIGURE 1. Diagram of Bayesian Optimization for PI controller.

A. Model of the Three-Phase Grid-Connected Converter

The Fig. 1 illustrates a grid-connected 3LNPC converter with a L filter. This type of converter uses an inductor (L_g) to smooth the current injected into the grid, reducing harmonics and minimizing electromagnetic disturbances. The simplicity of the L filter makes it a viable choice for low-power applications, ensuring an efficient connection between the converter and the electrical grid. However, due to its limited attenuation at high frequencies, system performance may be affected by oscillations and distortions, requiring advanced control strategies to optimize its operation [39].

The 3LNPC converter connected to the grid in three-phase systems can be represented as:

$$v_{a,NPC} = i_{g,a}R_g + L_g\frac{di_{a,g}}{dt} + v_{a,g}, \quad (1)$$

$$v_{b,NPC} = i_{g,b}R_g + L_g\frac{di_{b,g}}{dt} + v_{b,g}, \quad (2)$$

$$v_{c,NPC} = i_{g,c}R_g + L_g\frac{di_{c,g}}{dt} + v_{c,g}, \quad (3)$$

where the subscript NPC represents the 3LNPC converter, and g represents the grid, L_g and R_g represent, respectively, the inductance and internal resistance of the filter. The system representation in the synchronous reference frame can be reached by using coordinate transformation and it can be represented as:

$$\mathbf{v}_{NPC,dq} = \mathbf{i}_{g,dq}R_g + L_g\frac{d\mathbf{i}_{g,dq}}{dt} + \mathbf{v}_{g,dq} + j\omega_g L_g \mathbf{i}_{g,dq}, \quad (4)$$

which means

$$v_{NPC,d} = i_{g,d}R_g + L_g\frac{di_{g,d}}{dt} + v_{g,d} + \omega_g L_g i_{g,q}, \quad (5)$$

and

$$v_{NPC,q} = i_{g,q}R_g + L_g\frac{di_{g,q}}{dt} + v_{g,q} - \omega_g L_g i_{g,d}. \quad (6)$$

where $\mathbf{v}_{NPC,dq}$ express the converter voltage vector, $\mathbf{v}_{g,dq}$ represents the grid voltage vector, $\mathbf{i}_{g,dq}$ express the grid current vector and ω_g represents the grid angular frequency.

B. Grid Voltage Oriented Control for 3LNPC

Grid voltage-oriented control (VOC) is a strategy to ensure the stability and quality of electrical power in energy systems [40]. It operates by transforming the three-phase currents into a synchronous reference frame, aligned with the grid voltage vector—typically using a Phase-Locked Loop (PLL) [41]. In this case, it has a grid following operation. The Fig. 2 illustrates the VOC applied to the 3LNPC converter.

Initially, sensors measure the three-phase grid current, which is then converted into the $\alpha\beta$ reference frame using Clarke's transform [42]. Subsequently, the current is transformed into the synchronous reference frame dq based on the grid angle θ_g and the grid current vector. The angle θ_g is determined through measurements of the electrical grid voltage via sensors and processed using a PLL.

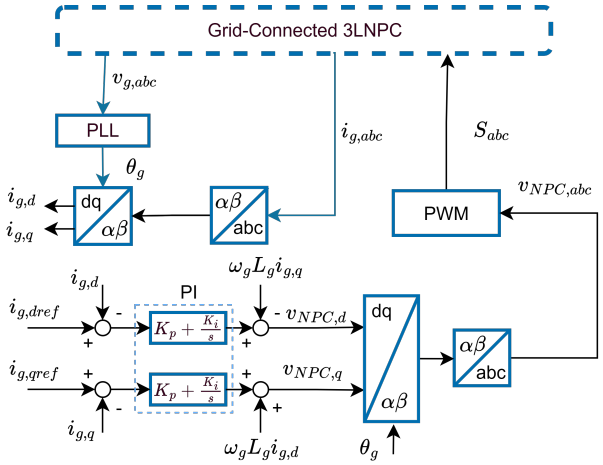

FIGURE 2. Diagram of VOC controller.

To regulate the system, two PI controllers compute the error between the grid current vector and its reference values, enabling the calculation of the converter voltage vector in the dq reference frame, as shown in Eq. (7) and (8). The PWM algorithm then generates control signals for the converter, utilizing the elements of the grid voltage vector in the stationary reference frame while employing the grid angle for synchronization:

$$v_{NPC,d} = (i_{g,dref} - i_{g,d}) \cdot PI - \omega_g L_g i_{g,q}, \quad (7)$$

$$v_{NPC,q} = (i_{g,qref} - i_{g,q}) \cdot PI + \omega_g L_g i_{g,d}, \quad (8)$$

where $PI = K_p + \frac{K_i}{s}$.

The DC link voltage is manipulated by means of the direct axis component of the grid current grid vector ($i_{g,d}$). In this case, the DC link voltage is represented by a fixed voltage source, and the reference current ($i_{g,dref}$) is directly supplied to the controller.

Therefore, proper tuning of the PI controller is essential to ensure system stability and efficiency, minimizing errors and improving dynamic response. Precise gain adjustment enables better control of the DC link voltage and grid current, ensuring reliable operation and high power quality.

C. Tune PI Controller using Byesian Optimization (BO)

Bayesian optimization is an efficient method for optimizing objective functions that are expensive to evaluate and lack an explicit structure. Initially, a set of points is selected and used to train a surrogate model, usually a Gaussian process [35]. This probabilistic model provides an estimate of the objective function and its uncertainty. At each iteration, an acquisition function is computed to determine the next evaluation point, maximizing a criterion such as exploration or exploitation. The chosen point is evaluated in the objective function and incorporated into the dataset, updating the surrogate

model. This process repeats until the maximum number of iterations or another stopping criterion is reached, returning the best solution found. The Bayesian approach enables an efficient exploration of the search space, making it ideal for optimizations where evaluations are limited or costly [36].

The PI controller adjusts the system current by comparing the measured value ($i_{g,dq}$) with the reference value ($i_{g,dqref}$) and applying corrections based on two terms: the proportional (K_p), which reacts instantly to the difference between the actual and desired value, and the integral (K_i), which accumulates errors over time to eliminate persistent deviations. This comparison is essential to minimize harmonic distortions, improve grid stability, and ensure compliance with power quality standards.

One of the criteria used to assess the quality of current control is the Integral of the Squared Error (ISE) [43]. The ISE computes the sum of errors over time, squaring them to penalize more significant deviations. An efficient controller should minimize this index, ensuring that the current quickly approaches the desired value and reducing the effects of oscillations and external disturbances. The use of ISE allows for comparisons between different control strategies, helping to select the one that provides the best system performance. In the case of current control, the ISE_{dq} for currents i_d and i_q can be calculated as follows:

$$ISE_{dq} = \sqrt{\int_0^T (i_{g,refd} - i_{g,d})^2 + (i_{g,refq} - i_{g,q})^2 dt}, \quad (9)$$

where T is the final time of the ISE analysis. As an iterative process, Bayesian Optimization can identify multiple sets of gains that result in a lower ISE. However, other performance parameters must be considered to ensure proper controller tuning. Thus, the following constraints were adopted: overshoot below ten percent ($Os_d < 10\%$) and settling time under three milliseconds ($St_d < 3$ ms), both for the step applied to the direct axis current. Therefore, the optimization problem for PI controller tuning using Bayesian Optimization can be defined as:

$$\begin{aligned} &\min_{x \in \mathcal{X}} f(x) = \text{minimize}(ISE_{dq}) \\ &\text{subject to: } Os_d < 10\% \text{ and } St_d < 3 \text{ ms}, \end{aligned} \quad (10)$$

where $\mathcal{X}$ is the search space containing possible values for the gains K_p and K_i.

Thus, the optimization process selects initial values of K_p and K_i from the search space $\mathcal{X}$, executes the model presented in Fig. 2 using a system simulation, calculates the ISE, adjusts the surrogate model, applies an acquisition function to select the next point to be evaluated, and repeats the process until the stopping criterion is met [44]. In this study, the chosen stopping criterion was the number of iterations ($n = 100$). At the end of the process, the values of K_p and K_i that meet the established performance criteria are verified. Fig. 3 illustrates the described process.

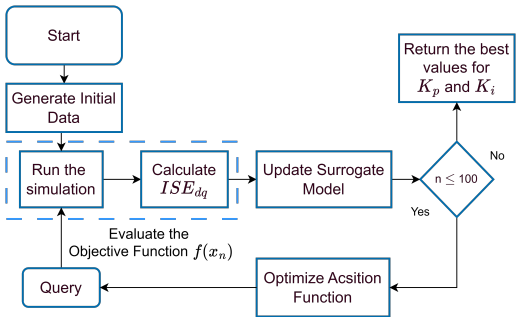

FIGURE 3. Bayesian Optimization for PI tune.

The optimization process described was performed using the bayesopt function in MATLAB and was configured with the parameters presented in Table 1.

TABLE 1. Parameters of Bayesian Optimization configuration.

Bayesian Optimization Configuration	
Searching Space $\mathcal{X}$	$K_p \in \mathbb{R}$, $1 \leq K_p \leq 1000$
	$K_i \in \mathbb{R}$, $1 \leq K_i \leq 1000$
Acquisition Function	Expected Improvement-Plus
Stopping Criterion	Number of iterations: n = 100
Random Seed (rng)	Default

III. EXPERIMENTAL SETUP

The simulations were conducted using MATLAB/Simulink on a workstation equipped with sufficient computational resources to support optimization algorithms and dynamic system modeling. The system configuration ensures reliable performance and numerical stability throughout the simulation process. Table 2 presents the described setup.

TABLE 2. Simulation Setup Specifications

Component	Specification
Processor	Intel Core i7-12700 (12th Gen), 2.10 GHz
RAM	16 GB (usable: 15.7 GB)
System Architecture	64-bit, x64-based processor
Operating System	Windows 11
MATLAB Version	R2024a

The test bench is designed to evaluate the performance of the proposal, which consists of an Imperix B-Box RCP system operating with Simulink-based control algorithms. The system is capable of sampling signals at a rate of 20 kHz, with data recorded through the Imperix Cockpit for accurate analysis. To simulate real-world conditions, a 9 kVA regenerative grid simulator is employed, functioning as an AC grid. The maximum output power of the multilevel converter employed in this study is rated at 23 kVA. Additionally, an L-filter with parameters $R_g = 23.9\ m\Omega$ and $L_g = 2.2\ mH$. This setup enables comprehensive testing and validation of the control strategies implemented within the B-Box RCP system, ensuring reliability and efficiency in various operational scenarios.

The laboratory setup employed to test the PI control is presented in Figs. 4.

FIGURE 4. Experimental platform used for control tests, composed of: converters, sensing and signal conditioning boards, Imperix B-Box RCP connected to a computer.

IV. RESULTS

The simulation phase aims to assess the effectiveness of Bayesian Optimization (BO) in determining the optimal tuning gains for the PI controller. The performance of the BO algorithm is benchmarked against the Genetic Algorithm (GA), focusing on convergence speed and the ability to explore the predefined search space. Furthermore, the PI controller tuned via BO is subjected to parametric variation and harmonic distortion tests to evaluate its robustness under dynamic operating conditions. The experimental tests are conducted on the setup described in Section III, with the objective of comparing the dynamic performance and power quality of the PI controller tuned via BO against controllers configured using empirical methods, specifically the Symmetrical Optimum (SO) and Yazdani approaches.

A. Simulation Results

Once the search space and Bayesian Optimization (BO) configurations were defined, as detailed in Section II, the optimization algorithm was employed to determine the tuning gains of the PI controller using the system simulation illustrated in Fig. 1. For comparative purposes, the Genetic Algorithm (GA) was also applied to the same tuning task. The GA was configured with MaxGenerations = 3, PopulationSize = 20, and EliteCount = 0, ensuring a total of 100 iterations—matching the number of evaluations used in the BO procedure. This population size was deliberately chosen to align the GA's evaluation budget with that of BO, so that both methods could be compared under equivalent computational effort. All other parameters were retained at their default values as defined by the Genetic Algorithm function within MATLAB's Global Optimization Toolbox. Fig. 5 presents the optimization results obtained from both algorithms.

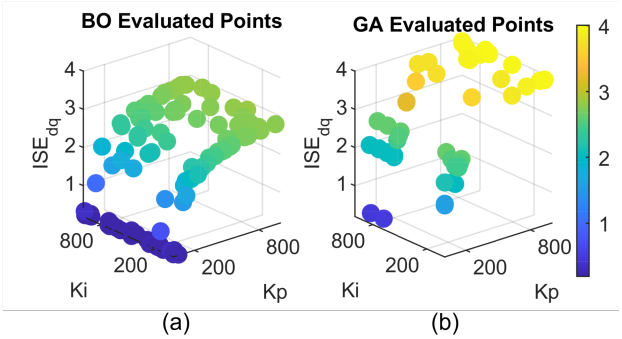

FIGURE 5. (a) Evaluated points of Bayesian Optimization. (b) Evaluated points of genetic algorithm.

Fig. 5 illustrates the optimization performance of Bayesian Optimization (BO) and the Genetic Algorithm (GA) in the search for optimal PI controller gains. In Fig. 5(a), the BO approach yields a significantly higher density of solutions where the ISE_{dq} is below 1, indicating superior tuning performance across a broader region of the search space. In contrast, Fig. 5(b) shows that the GA produces fewer optimal gain sets and exhibits a high repetition of explored points within the same 100 iterations. This behavior is consistent with the inherent characteristics of GA, which relies on population-based selection and crossover mechanisms that can lead to premature convergence and reduced diversity. Overall, the BO method demonstrates a more effective exploration of the search space, resulting in a richer set of high-performance controller configurations, as evidenced by the convergence behavior of the cost function over 100 iterations illustrated in Fig. 6. This highlights the method's ability to balance exploitation and exploration, ultimately leading to more robust and diverse controller designs.

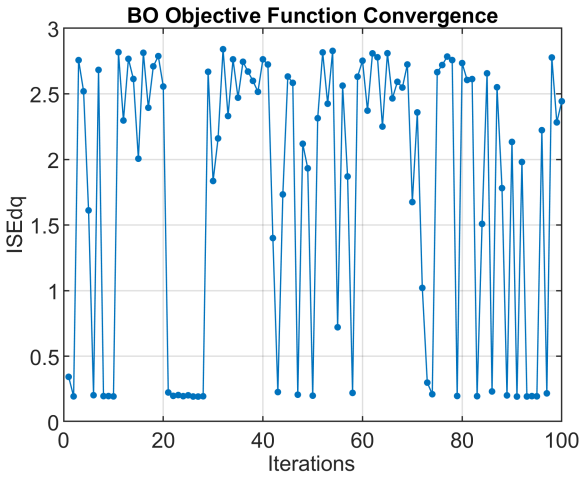

FIGURE 6. BO Objective Function Convergence.

In terms of computational time, the Genetic Algorithm (GA) required approximately 72.7 minutes (4359.36 seconds) to complete 100 iterations, while Bayesian Optimization (BO) completed the same number of evaluations in

approximately 67.9 minutes (4073.40 seconds). Although BO was slightly faster, the difference in execution time is not substantial and does not significantly impact the overall feasibility of either method. It is important to note that the GA is particularly sensitive to the population size parameter. Larger populations tend to improve the diversity of candidate solutions and reduce the risk of premature convergence, but they also increase computational cost, as presented in [22]. Conversely, smaller populations may lead to faster execution but can compromise the quality and diversity of the solutions found. Therefore, careful tuning of the population size is essential to balance performance and efficiency in GA-based optimization.

After the iterations, the tuning point with the lowest ISE_{dq}, overshoot below ten percent ($Os_d < 10\%$), and settling time under three milliseconds ($St_d < 3$ ms) was selected. As a reference, to evaluate the performance of the PI controller tuned using BO, the controller was also configured using two classical methods: the Symmetrical Optimum (SO) and the method proposed in [17] (Yazi). The selected gains for all three methods are presented in Tab.3.

TABLE 3. Gains found for each evaluated method.

Tune Method	K_p	K_i
Bayesian Optimization	22.79	489.54
Symmetrical Optimum	11	13750
Yazdani	44	467.8

To evaluate the robustness of the controller tuned using the proposed method, parametric variation tests were performed by individually adjusting the values of R_g and L_g from 50% to 150% of their nominal references, as shown in Table 5 and 4. The results indicate that the controller is capable of maintaining power quality under reduced Lg conditions, achieving total harmonic distortion (THD) below 5%. However, this scenario leads to slower dynamic response and increased overshoot. In contrast, variations in Rg did not produce significant changes in the controller's behavior, suggesting low sensitivity to grid resistance fluctuations.

TABLE 4. Parametric variation settings of the grid inductance (L_g) applied for evaluating the robustness of the controller.

Lg = 2.2 mH	ISE_{dq}	Os_d (%)	St_d (ms)	THD (%)
50%	0.356	31.87	67.30	2.22
62.5%	0.290	23.35	44.00	1.81
75%	0.248	12.82	0.23	1.56
87.5%	0.220	11.87	0.28	1.34
100%	0.200	6.96	0.18	1.29
112.5%	0.188	5.48	0.20	1.25
125%	0.180	5.88	0.23	1.25
137.5%	0.174	6.00	0.29	1.24
150%	0.171	6.01	0.28	1.27

TABLE 5. Parametric variation settings of the grid resistence (R_g) applied for evaluating the robustness of the controller.

Rg = 23.29 mΩ	ISE_{dq}	Os_d (%)	St_d (ms)	THD (%)
50%	0.200	6.00	0.19	1.28
62.5%	0.201	5.95	0.18	1.31
75%	0.200	5.97	0.18	1.30
87.5%	0.201	5.46	0.19	1.32
100%	0.200	6.96	0.18	1.29
112.5%	0.201	5.42	0.18	1.27
125%	0.201	5.51	0.18	1.32
137.5%	0.201	6.0	0.19	1.29
150%	0.201	5.57	0.18	1.30

Additionally, to further evaluate the robustness of the PI controller beyond parametric variations, harmonic distortion tests were conducted under more challenging grid conditions. These tests aimed to assess the controller's ability to maintain power quality when subjected to distorted voltage waveforms. The distorted grid scenario is based on the configuration presented in [45], where the voltage includes a 60 Hz fundamental component along with harmonic components of the 5th (3.94%), 7th (3.15%), 11th (2.36%), 13th (1.5%), 17th (1.1%), and 19th (0.7%) orders, with respective amplitudes shown in parentheses. This harmonic profile results in a total harmonic distortion (THD) of approximately 6%, providing a realistic nonideal operating condition for evaluating the controller's performance. The dynamic behavior of the system under this distorted grid scenario is illustrated in Fig. 7, which highlights the controller's ability to mitigate harmonic effects and maintain power quality.

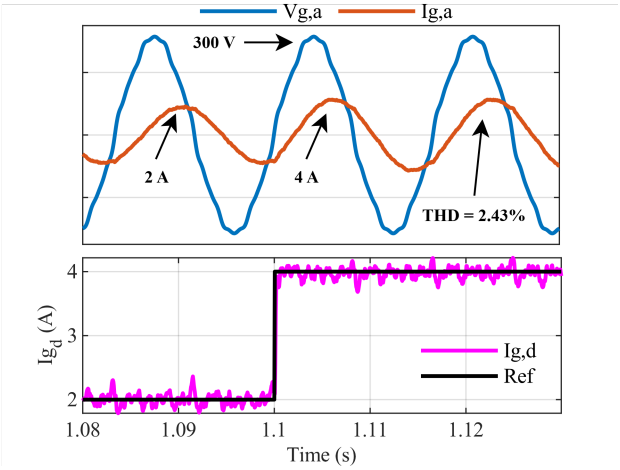

FIGURE 7. Simulation results under harmonic distortion conditions.

B. Experimental Results

The dynamic response of the controller was tested using the experimental setup described in the previous section. The grid to which the converter is connected operates with a phase-to-phase voltage of 380 V and a frequency of 60 Hz.

The controller's performance was evaluated by applying step signals to the $i_{g,d}$ and $i_{g,q}$ components of the current. For the $i_{g,d}$ component, the reference current is initialized at 0 A. The first step is applied at 0.1 s, raising the reference to 2 A. Subsequently, at 1.1 s, a second step increases the current to 4 A. The current returns to 2 A at 2.1 s and is finally reduced to 0 A at 3.1 s. For the $i_{g,q}$ component, the reference also starts at 0 A. At 0.6 s, a negative step is applied to -2 A, followed by a second step at 0.9 s reducing the current further to -4 A. The current returns to 0 A at 2.6 s. Figure 8 illustrates the response of the controller tuned using BO for the reference steps described above. The performance demonstrates that the controller's response follows the reference for both components.

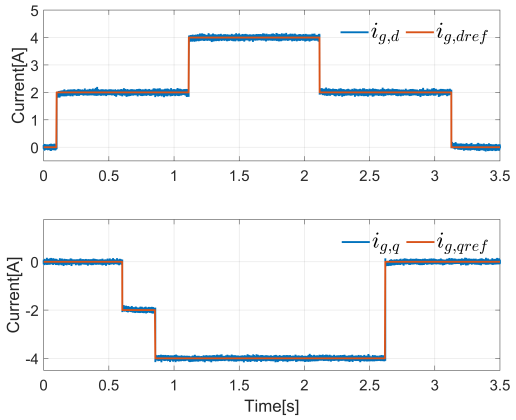

FIGURE 8. Dynamic response of the PI control tuned by BO for $i_{g,d}$ and $i_{g,q}$ steps.

Fig. 9 shows the three-phase currents following the step applied to $i_{g,d}$ at 1.1 seconds. A change in current amplitude from 4 A to 6 A can be observed, resulting from the combined contributions of the $i_{g,d}$ and $i_{g,q}$ components.

Fig. 10 shows the behavior of the voltage $v_{g,a}$ and current $i_{g,a}$ in response to the controller's action following the step applied to $i_{g,d}$ at 0.1 seconds. The observed behavior indicates that the current remains in phase with the voltage, as the reference for the $i_{g,q}$ component is held at zero throughout this interval. This implies that there is no reactive power contribution, resulting in a purely active power flow aligned with the grid voltage waveform.

Fig.11 illustrates the step applied to the $i_{g,d}$ reference at 1.1 seconds and the corresponding control response for the three evaluated tuning methods. Based on the observed performance, the controller tuned with Yazdani's (Yazi) exhibited the shortest rise time ($Rt_d = 0.063$ ms) but also the highest overshoot among the evaluated methods ($Os_d = 44.22\%$). The tuning based on Symmetrical Optimum (SO) resulted in the longest rise time ($Rt_d = 0.28$ ms), the longest settling time ($St_d = 1.3$ ms), and a significant overshoot ($Os_d = 20\%$). Meanwhile, the controller optimized using Bayesian Optimization showed the second shortest rise time ($Rt_d = 0.136$ ms), the shortest settling time ($St_d = 0.249$

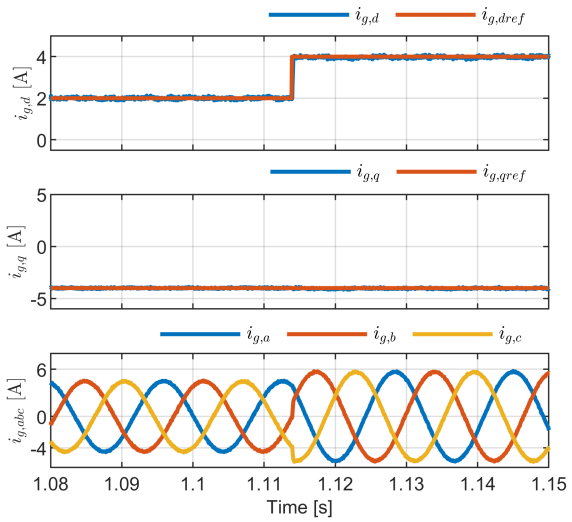

FIGURE 9. Three-phase current of the dynamic response of the PI controller tuned by BO.

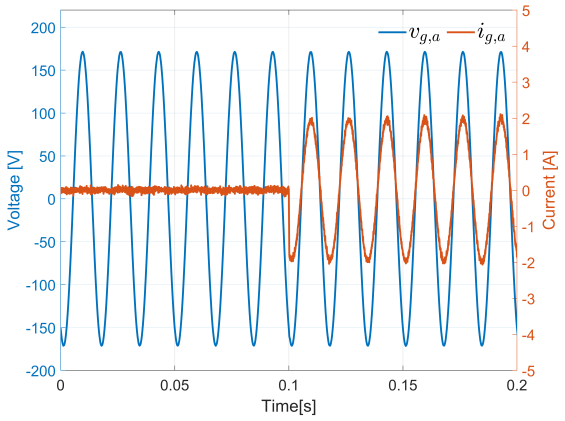

FIGURE 10. Phase a current and voltage of the dynamic response of the PI controller tuned by BO.

ms), and an overshoot below 5% ($Os_d = 3.7\%$), demonstrating the best dynamic performance among the three evaluated tuning methods. The values mentioned are presented in Table 6 to facilitate comparison among the evaluated tuning methods.

TABLE 6. Dynamic response values for $i_{g,d}$ step of tune methods.

Tune Method	Os_d (%)	Rt_d (ms)	St_d (ms)
Bayesian Optimization	3.711	0.136	0.249
Symmetrical Optimum	20.00	0.284	1.3
Yazdani	44.22	0.063	0.451

Fig. 12 illustrates the step change in the $i_{g,q}$ reference at 2.6 seconds and the corresponding control response for the three evaluated tuning methods. The behavior observed is similar to that seen in the $i_{g,d}$ step response, with the optimized tuning method demonstrating the best performance

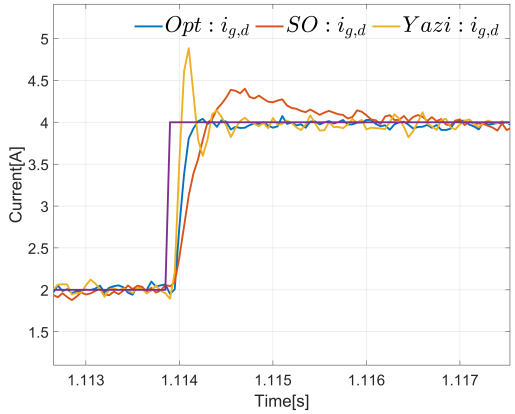

FIGURE 11. Dynamic response of the PI control for i_d step with each tune method.

among the evaluated approaches. The performance values are presented in Table 7 to facilitate comparison among the evaluated tuning methods.

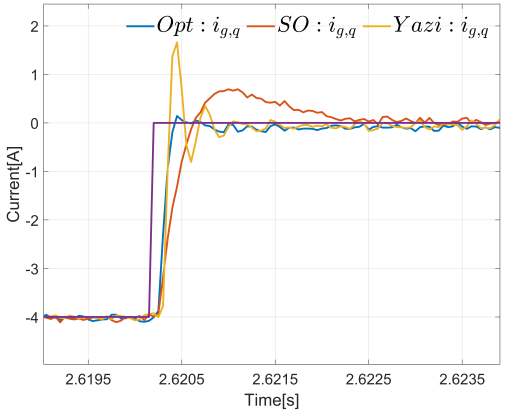

FIGURE 12. Dynamic response of the PI control for $i_{g,q}$ step with each tune method.

TABLE 7. Dynamic response values for $i_{g,q}$ step of tune methods.

Tune Method	Os_q (%)	Rt_q (ms)	St_q (ms)
Bayesian Optimization	3.563	0.127	0.235
Symmetrical Optimum	17.34	0.285	1.5
Yazdani	41.49	0.058	0.448

In addition to the analysis of the dynamic response, the ISE_{dq} index and Total Harmonic Distortion (THD) was computed for all evaluated controllers. The results presented in Table 8 indicate that the controller configured using the proposed tuning methodology achieves the lowest integral of squared error across both current components, highlighting its superior tracking performance. The THD values obtained by the controllers tuned with the three evaluated methods comply with the international IEEE 1547.2-2008 standard, remaining below 5%. Moreover, the controller tuned with BO achieves the lowest THD, with a value of 1.05%.

TABLE 8. ISE_{dq} and THD (%) for each tune method.

Tune Method	ISE_{dq}	THD (%)
Bayesian Optimization	0.1334	1.05
Symmetrical Optimum	0.1536	1.29
Yazdani	0.1568	1.17

V. CONCLUSION

Thus, this work demonstrates that Bayesian Optimization (BO) offers superior performance in exploring the search space when tuning the gains of the PI controller for the three-level 3LNPC converter. Unlike classical methods, BO efficiently identifies promising regions by leveraging probabilistic models, resulting in a broader and more effective coverage of the solution space. Even with a fixed limit of 100 iterations—equal to that used for the Genetic Algorithm (GA)—BO produced a greater number of viable solutions that met the control performance criteria. This enhanced exploration capability allowed for a more comprehensive understanding of parameter sensitivity and system behavior. The PI controller tuned with BO reliably tracked the desired reference, exhibiting low overshoot ($< 5\%$) and a settling time below 3 ms. Additionally, compliance with the IEEE 1547.2-2008 standard was confirmed, with current harmonics remaining under 5%. These findings establish BO as a robust and promising alternative for integration into power generation systems based on three-level converters, offering improved reliability and control precision.

ACKNOWLEDGMENT

This study could not be conducted without the physical structure and funding provided by the USP (University of São Paulo), FAPESP (São Paulo state foundation for research support) Project 2025/07022-7 and 2025/05229-3, CNPq (scientific development national council) Project 407867/2022-8 and 444259/2024-4 and CAPES (Coordination for the Improvement of Higher Education Personnel – Brazil) Project 001. Special thanks for the RCGI (Research Centre for Greenhouse Gas Innovation) and Total Energies, funding the projects ANP (National Petroleum and Gas Agency) 23673-7 (6) and 23658-8 (5).

AUTHOR'S CONTRIBUTIONS

V.S.JORGE: Conceptualization, Data Curation, Investigation, Methodology, Software, Validation, Writing – Original Draft, Writing – Review & Editing. **A.S.LUNARDI:** Data Curation, Formal Analysis, Resources, Software, Supervision, Writing – Original Draft, Writing – Review & Editing. **L.A.SOUSA:** Validation. **R.V.ROCHA:** Conceptualization, Investigation, Writing – Original Draft. **R.M.MONARO:** Project Administration, Resources, Supervision. **A.J.S.FILHO:** Conceptualization, Project Admin-

istration, Resources, Supervision, Visualization, Writing – Review & Editing.

PLAGIARISM POLICY

This article was submitted to the similarity system provided by Crossref and powered by iThenticate – Similarity Check.

DATA AVAILABILITY

The data used in this research is available in the body of the document.

REFERENCES

[1] V. Yaramasu, B. Wu, P. C. Sen, S. Kouro, M. Narimani, "High-power wind energy conversion systems: State-of-the-art and emerging technologies", *Proceedings of the IEEE*, vol. 103, no. 5, pp. 740–788, may 2015, doi:10.1109/JPROC.2014.2378692.

[2] M. Abbes, J. Belhadj, "New control method of a robust NPC converter for renewable energy sources grid connection", *Electric Power Systems Research*, vol. 88, pp. 52–63, 2012, doi:10.1016/j.epsr.2012.01.018.

[3] B. Malakondareddy, S. Senthil Kumar, N. Ammasai Gounden, I. Anand, "An adaptive PI control scheme to balance the neutral-point voltage in a solar PV fed grid connected neutral point clamped inverter", *International Journal of Electrical Power and Energy Systems*, vol. 110, no. October 2018, pp. 318–331, 2019, doi:10.1016/j.ijepes.2019.03.012.

[4] A. Yazdani, R. Iravani, "A neutral-point clamped converter system for direct-drive variable-speed wind power unit", *IEEE Transactions on Energy Conversion*, vol. 21, no. 2, pp. 596–607, 2006, doi:10.1109/TEC.2005.860392.

[5] M. Seixas, R. Melício, V. M. Mendes, "Offshore wind turbine simulation: Multibody drive train. Back-to-back NPC (neutral point clamped) converters. Fractional-order control", *Energy*, vol. 69, pp. 357–369, 2014, doi:10.1016/j.energy.2014.03.025.

[6] F. Rojas, R. Cardenas, R. Kennel, J. C. Clare, M. Diaz, "A Simplified Space-Vector Modulation Algorithm for Four-Leg NPC Converters", *IEEE Transactions on Power Electronics*, vol. 32, no. 11, pp. 8371–8380, 2017, doi:10.1109/TPEL.2016.2618061.

[7] N. S. Hasan, N. Rosmin, D. A. A. Osman, A. H. Musta'amal Jamal, "Reviews on multilevel converter and modulation techniques", *Renewable and Sustainable Energy Reviews*, vol. 80, no. May, pp. 163–174, 2017, doi:10.1016/j.rser.2017.05.163.

[8] M. Porru, A. Serpi, I. Marongiu, A. Damiano, "Suppression of DC-link voltage unbalance in three-level neutral-point clamped converters", *Journal of the Franklin Institute*, vol. 355, no. 2, pp. 728–752, 2018, doi:10.1016/j.jfranklin.2017.11.039.

[9] J. Hu, Y. Shan, J. M. Guerrero, A. Ioinovici, K. W. Chan, J. Rodriguez, "Model predictive control of microgrids – An overview", *Renewable and Sustainable Energy Reviews*, vol. 136, 2 2021, doi:10.1016/j.rser.2020.110422.

[10] J. Liu, Y. Miura, T. Ise, "Cost-Function-Based Microgrid Decentralized Control of Unbalance and Harmonics for Simultaneous Bus Voltage Compensation and Current Sharing", *IEEE Transactions on Power Electronics*, vol. 34, pp. 7397–7410, 2019, doi:10.1109/TPEL.2018.2879340.

[11] L. Meegahapola, A. Sguarezi, J. S. Bryant, M. Gu, E. R. Conde D., R. B. A. Cunha, "Power System Stability with Power-Electronic Converter Interfaced Renewable Power Generation: Present Issues and Future Trends", *Energies*, vol. 13, no. 13, 2020, doi:10.3390/en13133441.

[12] A. Lunardi, L. F. Normandia Lourenço, E. Munkhchuluun, L. Meegahapola, A. J. Sguarezi Filho, "Grid-Connected Power Converters: An Overview of Control Strategies for Renewable Energy", *Energies*, vol. 15, no. 11, p. 4151, 2022, doi:10.3390/en15114151.

[13] K. Ogata, *Engenharia de Controle Moderno*, 5ª ed., Pearson Education do Brasil, 2011.

[14] H. A. Young, M. A. Perez, J. Rodriguez, "Analysis of Finite-Control-Set Model Predictive Current Control With Model Parameter Mismatch in a Three-Phase Inverter", *IEEE Transactions on Industrial Electronics*, vol. 63, no. 5, pp. 3100–3107, 2016, doi:10.1109/TIE.2016.2515072.

[15] A. K. Mishra, S. M. Tripathi, O. Singh, A. K. Srivastava, T. Venkatraman, R. R. Vijayaraghavan, S. Kumar, R. M. Elavarasan, L. Mihet-Popa, "Performance assessment of VSC-based HVDC system in asynchronous grid interconnection: Offline and real-time validation of control design with symmetric optimum PI tuning", *Heliyon*, vol. 10, no. 15, p. e35624, 2024, doi:10.1016/j.heliyon.2024.e35624.

[16] L. Quéval, H. Ohsaki, "Back-to-back converter design and control for synchronous generator-based wind turbines", *in 2012 International Conference on Renewable Energy Research and Applications (ICRERA)*, pp. 1–6, 2012, doi:10.1109/ICRERA.2012.6477300.

[17] A. Yazdani, R. Iravani, *Voltage-sourced Converters in Power Systems - Modeling, Control, and Applications*, Willey, 2010, doi:10.1002/9780470551578.

[18] M. Ismail, R. Chibani, M. Hamouda, K. Al-Haddad, "Artificial neural network based auto-tuned PI compensator to enhance the dynamic response of the DC-link voltage in a grid-connected voltage source converter", *in 2022 IEEE 1st Industrial Electronics Society Annual On-Line Conference (ONCON)*, pp. 1–6, 2022, doi:10.1109/ONCON56984.2022.10126755.

[19] M. Rabosha, S. Rehimi, H. Bevrani, "Frequency and Active Power Control of Interconnected Microgrids: An ANN-Based PI Tuning Approach", *in 2024 14th Smart Grid Conference (SGC)*, pp. 1–6, 2024, doi:10.1109/SGC64640.2024.10983776.

[20] H. Rafia, H. Ouadi, B. El Bhiri, "ANN-PI Controller for the Grid-Side Converters in Wind Energy Conversions Systems under Voltage Dips", *IFAC-PapersOnLine*, vol. 58, no. 13, pp. 575–580, 2024, doi:10.1016/j.ifacol.2024.07.544, 12th IFAC Symposium on Control of Power and Energy Systems - CPES 2024.

[21] G. V. Hollweg, P. J. D. de Oliveira Evald, E. Mattos, L. C. Borin, R. V. Tambara, V. F. Montagner, "Self-tuning methodology for adaptive controllers based on genetic algorithms applied for grid-tied power converters", *Control Engineering Practice*, vol. 135, p. 105500, 2023, doi:10.1016/j.conengprac.2023.105500.

[22] L. Rodrigues, A. Potts, O. Vilcanqui, A. Sguarezi, "Tuning a model predictive controller for Doubly Fed Induction Generator employing a constrained Genetic Algorithm", *IET Electric Power Applications*, vol. 13, 05 2019, doi:10.1049/iet-epa.2018.5922.

[23] S. Tian, Y. Zhang, L. Liu, P. Su, B. Zou, "Analysis of PI Parameter Tuning for Offshore Wind Power Based on Improve Grey Wolf Optimization Algorithm", *in 2023 4th International Conference on Advanced Electrical and Energy Systems (AEES)*, pp. 679–683, 2023, doi:10.1109/AEES59800.2023.10469329.

[24] A. A. Al-Shamma'a, H. Olabisi Omotoso, A. M. Noman, A. A. Alkuhayli, "Grey Wolf Optimizer Based Optimal Control for Grid-Connected PV System", *in IECON 2020 The 46th Annual Conference of the IEEE Industrial Electronics Society*, pp. 2863–2867, 2020, doi:10.1109/IECON43393.2020.9254841.

[25] S. K, K. P. P, S. K, "Grey Wolf Optimized PI Controller for Grid Tied High Gain Converter for Solar Power Generation", *in 2023 International Conference on Integration of Computational Intelligent System (ICICIS)*, pp. 1–6, 2023, doi:10.1109/ICICIS56802.2023.10430247.

[26] A. Kumar, A. Alam, "Whale Optimization Algorithm in Grid-Connected Inverter with SRF-PI", *in 2022 IEEE 2nd International Conference on Sustainable Energy and Future Electric Transportation (SeFeT)*, pp. 1–6, 2022, doi:10.1109/SeFeT55524.2022.9909388.

[27] A. Chakraborty, T. Maity, "An enhanced Whale Optimization Algorithm based Control Strategy for LVRT Capability Enhancement of Grid-Connected DFIG-WECS", *in 2022 IEEE 19th India Council International Conference (INDICON)*, pp. 1–6, 2022, doi:10.1109/INDICON56171.2022.10040151.

[28] B. Mothi Ram, A. Ganesh, "Optimal Voltage Imbalance Compensation in Islanded Microgrid by Using Whale Optimization Technique", *in 2021 7th International Conference on Electrical Energy Systems (ICEES)*, pp. 484–489, 2021, doi:10.1109/ICEES51510.2021.9383703.

[29] C. Sreenu, G. Mallesham, T. C. Shekar, S. R. Salkuti, "Pairing voltage-source converters with PI tuning controller based on PSO for grid-connected wind-solar cogeneration", *Franklin Open*, vol. 8, p. 100138, 2024, doi:10.1016/j.fraope.2024.100138.

[30] M. W. Alzahlan, K. M. Alawasa, H. D. Al-Majali, "Performance Evaluation of Different Optimal-Tuned Current Controllers for Voltage-Source Converter Connected to a Weak AC Grid", *in 2019 IEEE Jordan International Joint Conference on Electrical Engineering and Information Technology (JEEIT)*, pp. 198–203, 2019, doi:10.1109/JEEIT.2019.8717376.

[31] L. L. Rodrigues, J. S. Solís-Chaves, O. A. C. Vilcanqui, A. J. S. Filho, "Predictive Incremental Vector Control for DFIG With Weighted-Dynamic Objective Constraint-Handling Method-PSO Weighting Matrices Design", *IEEE Access*, vol. 8, pp. 114112–114122, 2020, doi:10.1109/ACCESS.2020.3003285.

[32] G. A. Ghazi, E. A. Al-Ammar, H. M. Hasanien, R. A. Turky, "Transient Search Optimization Based Fuzzy-PI Controller for MPPT of Standalone PV System", *in 2022 23rd International Middle East Power Systems Conference (MEPCON)*, pp. 1–5, 2022, doi:10.1109/MEPCON55441.2022.10021781.

[33] Z. Chen, R. Zheng, R. Ma, S. Li, Y. Li, M. Cui, Y. Yang, "Comparison of PID Controllers with Engineering-Tuned Parameters and Fuzzy PID Controllers in the Application of Boost Converters", *in 2024 3rd International Conference on Energy, Power and Electrical Technology (ICEPET)*, pp. 1824–1829, 2024, doi:10.1109/ICEPET61938.2024.10627733.

[34] K. A. C. Chirapo, S. G. Di Santo, A. Sguarezi, I. Delgado, "Direct power control of 12/8 Switched Reluctance Generator connected to single-phase electrical grid using the self-tuning FUZZY PI Controller", *in 2019 IEEE XXVI International Conference on Electronics, Electrical Engineering and Computing (INTERCON)*, pp. 1–4, 2019, doi:10.1109/INTERCON.2019.8853576.

[35] W. Stróżecki, N. A. Oufroukh, Y. Kebbati, D. Ichalal, S. Mammar, "Automatic Tuning of MPC for Autonomous Vehicle using Bayesian Optimization", *in 2021 IEEE International Conference on Networking, Sensing and Control (ICNSC)*, vol. 1, pp. 1–6, 2021, doi:10.1109/ICNSC52481.2021.9702240.

[36] A. V. Richter, J. D. le Roux, I. K. Craig, "Bayesian optimization for automatic tuning of a MIMO controller of a flotation bank", *Journal of Process Control*, vol. 147, p. 103388, 2025, doi:10.1016/j.jprocont.2025.103388.

[37] Z. Liu, L. Li, "Controller tuning via constrained Bayesian optimization", *in 2024 5th International Conference on Computer Engineering and Application (ICCEA)*, pp. 1469–1472, 2024, doi:10.1109/ICCEA62105.2024.10603844.

[38] F. A. Almasalmah, H. Omran, C. Liu, T. Poignonec, B. Bayle, "Auto-Tuning of Model Predictive Control for Bilateral Teleoperation with Bayesian Optimization", *IFAC-PapersOnLine*, vol. 58, no. 30, pp. 85–90, 2024, doi:10.1016/j.ifacol.2025.01.161, 5th IFAC Workshop on Cyber-Physical Human Systems.

[39] A. F. Precht, B. E. Recktenvald, A. C. K. Filho, P. C. Bolsi, E. O. Prado, H. C. Sartori, J. R. Pinheiro, "A Comparative Analysis of L and LCL Filters in Grid-Connected Converters Regarding Volume and Losses", *in 2023 15th Seminar on Power Electronics and Control (SEPOC)*, pp. 1–6, 2023, doi:10.1109/SEPOC58810.2023.10322611.

[40] K. Matiyali, S. Goel, H. Joshi, "Voltage Oriented Control of Grid-tied Solar PV System", *in 2019 Women Institute of Technology Conference on Electrical and Computer Engineering (WITCON ECE)*, pp. 28–34, 2019, doi:10.1109/WITCONECE48374.2019.9092933.

[41] W. Ouyang, Y. Zhu, W. Zhang, Z. Wang, "Comparison of PLL and without PLL control for grid-connected VSCs under large disturbances", *in 2024 IEEE 7th International Electrical and Energy Conference (CIEEC)*, pp. 4010–4015, 2024, doi:10.1109/CIEEC60922.2024.10583342.

[42] D. Bellan, "Transient Analysis of Single-Line-to-Ground Faults in Three-Phase Circuits Using Clarke Transformation", *in 2018 International Conference and Utility Exhibition on Green Energy for Sustainable Development (ICUE)*, pp. 1–4, 2018, doi:10.23919/ICUE-GESD.2018.8635674.

[43] J. S. Costa, A. Lunardi, A. J. S. Filho, "MPC design control modulation using performance map applied to VCS-grid converter with L filter", *Eletrônica de Potência*, vol. 27, 12 2022, doi:10.18618/REP.2022.4.0014.

[44] N. Rontsis, M. A. Osborne, P. J. Goulart, "Distributionally Ambiguous Optimization for Batch Bayesian Optimization", *Journal of Machine Learning Research*, vol. 21, no. 149, pp. 1–26, 2020, URL: http://jmlr.org/papers/v21/18-211.html.

[45] J. S. Costa, A. Lunardi, L. F. Normandia Lourenço, I. Oliani, A. J. Sguarezi Filho, "Lyapunov-Based Finite Control Set Applied to an EV Charger Grid Converter Under Distorted Voltage", *IEEE Transactions on Transportation Electrification*, vol. 11, no. 1, pp. 3549–3557, 2025, doi:10.1109/TTE.2024.3443691.

BIOGRAPHIES

Vitor S. Jorge Received a B.Sc degree in Electrical Engineering from the Federal University of Pará (UFPA) in Tucuruí, Pará, Brazil, in 2022, and a M.S degree in Applied Computing from the same institution in 2025. Currently pursuing a Ph.D. in the Energy graduate program at the Federal University of ABC (UFABC), Santo André, São Paulo, Brazil. His research interests include control applied to machine drives, power converters and wind energy.

Angelo S. Lunardi received the degree in electronic engineering from the Instituto Mauá Tecnologia, in 2015, the master's degree in electrical engineering from the Universidade Federal do ABC (UFABC), with a focus on control research applied to wind power generation, in 2017, and the Ph.D. degree in electrical engineering from the University of São Paulo (USP) with a thesis titled robust predictive control applied to the converter connected to the grid, in 2022. Currently, he is a researcher at the UFABC and works with control systems for renewable energy.

Luan A. Sousa received the B.Sc. degree from the University of Sao Paulo, São Paulo, Brazil, in 2018. and the M.Sc. degree in 2022 from the University of Sao Paulo, São Paulo, Brazil. He is currently a researcher in a laboratory at the Inova USP building, Butantã campus, São Paulo, Brazil, where he conducts research in his areas of interest. His research interests include measuring and protection of power systems and distributed generation and renewable energy.

Rodolfo V. Rocha received the B.Sc. degree in electrical engineering from the Federal University of Mato Grosso, Cuiabá, Brazil, in 2013; the M.Sc. degree from the São Carlos School of Engineering, University of São Paulo, São Carlos, Brazil, in 2016; and the Ph.D. degree at the Polytechnic School of the University of São Paulo, São Paulo, Brazil, in 2023. He is currently an Adjunct Professor at the Federal University of Mato Grosso, Cuiabá, Brazil. His research interests include measuring, control and protection of power systems, electric machines and power converters.

Renato M. Monaro received the B.Sc. degree in electrical engineering from University of Sao Paulo, São Carlos, Brazil, in 2007. He received the Ph.D. degree from the same institution. At present, he is an Associate Professor at the University of São Paulo, São Paulo, Brazil. His main research interests include power system control and protection, HVDC-VSC transmission, distributed generation, and renewable energy.

Alfeu J. Sguarezi received his Master and Doctor degrees in Electrical Engineering from the Faculty of Electrical and Computer Engineering of the University of Campinas (Unicamp) in 2007 and 2010, respectively. Currently, he is Associate Professor at the Federal University of ABC (UFABC). He is a Senior Member of the IEEE and author of several articles in national and international scientific journals and book chapters in the areas of electrical machines, machine drives, electric vehicles, power electronics, and wind and photovoltaic energies.